Proceedings of 2022 IEEE
International Conference on Mechatronics and Automation
August 7 - 10, Guilin, China

A Novel Solar Tracker with a Foldable Solar Harvesting Mechanism for an Amphibious Robot

Chang Liu[1], Zhuowei Sun[1], Congyu Huang[1], Shunli Wang[1], Huiming Xing[1*], Shuxiang Guo[2], Wenzhi Liu[1], Haibo Li[1]

[1] *College of Intelligent Systems Science and Engineering, Harbin Engineering University, No.145, Nantong Street, Nangang District, Harbin 150001, Heilongjiang Province, China*

[2] *Key Laboratory of Convergence Medical Engineering System and Healthcare Technology, the Ministry of Industry and Information Technology, School of Life Science, Beijing Institute of Technology, Haidian District, Beijing 100081, China*

Chang Liu, Zhuowei Sun and Congyu Huang contributed equally to this paper.
Corresponding author's e-mails: xinghuiming@hrbeu.edu.cn

***Abstract* – Inspired by the solar tracking mechanism that the sunflower can adjust the attitude of its flower disk towards the sun for maximum power efficiency, this paper proposed a novel solar tracker method with a foldable solar harvesting mechanism for an amphibious robot. Using ADAMS simulation, the driving torques of solar panels are generated for servomotors selection and this foldable mechanism is optimized. Using the control of four servomotors, four solar panels is folded up one by one. The fordable compact mechanism can reduce the water resistance and the influence of water flow and improve power harvesting efficiency. With the desired attitude calculated by the robot local position and time, the robot adjusts the attitude of the solar panels towards the sun for maximum power efficiency. Based on the dynamic model of the robot, the attitude control method is developed. Finally, experiments with the robot attitude adjustment were conducted using the robot prototype. Compared with no attitude adjustment, the solar energy harvesting efficiency is improved by 62.4%, which proved the feasibility of the proposed solar tracker.**

Index Terms – amphibious robots; solar tracker; foldable solar harvesting mechanism

I. Introduction

Currently, the energy is one of the most limitation to underwater robots and vehicles for these high-risk tasks, such as pollution detection, resource exploration, environmental monitoring, scientific research and personnel search and rescue. In order to extend the working area of the robot, many researchers focused on the self-charging technology and many methods for developing self-powered technology are proposed to collect energy from the surrounding marine environment, such as wind, ocean wave and ocean thermal energy. In order to make full use of these forms of energy, researchers have put forward many schemes.

In terms of wave energy collection, a variety of piezoelectric energy collectors that can convert wave energy into electrical energy have been proposed. Hwang *et al*. proposed a piezoelectric wave energy collector using rocking motion [1]. Viet *et al*. proposed a floating energy collector for obtaining energy from deep water waves [2]. Chen *et al.* studied a nonlinear piezoelectric energy collector to improve efficiency and bandwidth [3]. Nabavi *et al.* proposed a new piezoelectric buoy energy acquisition device [4]. Peng *et al.* proposed a compression piezoelectric generator composed of piezoelectric stack and spring mass system [5]. Nie *et al.* proposed a broadband piezoelectric vibration energy collector [6]. In addition, many electromagnetic transducers and electromagnetic energy collectors are proposed, which can convert kinetic energy into electrical energy. Masoumi *et al.* proposed a variable resonant wave energy collector based on repulsive magnetic levitation [7]. Prudell *et al*. proposed a permanent magnet tubular linear generator for wave energy conversion [8]. Li *et al*. proposed a parallel hybrid excitation linear vernier machine (PHE-LVM) for directly driving wave power generation [9]. Hodgins *et al*. proposed a linear wave energy generator [10]. Rhinefrank et al. studied a novel permanent magnet linear generator buoy using marine energy[11]. In terms of wind energy collection, Zhao *et al*. proposed a novel water-proof hybrid wind energy harvester (WP-HWH) [12]. Na *et al*. proposed a novel wind energy harvester based on a magneto-piezo-elastic structure [13]. Rahman *et al*. proposed a natural wind-driven ultra-compact and highly efficient hybridized nanogenerator [14]. In terms of ocean thermal energy collection, Wang *et al.* proposed a new design of underwater glider driven by temperature difference energy [15].

The above literatures achieve the significant progress of self-powered supply technology. However, in terms of the amphibious environment and the power demand of the robot, the large devices of these schemes have low conversion efficiency. The power generated is not enough for battery charging, and it is difficult to be embedded into the underwater robot system. These methods cannot well solve the energy problem of the amphibious robots [16-18, 25-34] in the complex amphibious environment.

Solar energy is a widely distributed and renewable energy. Solar charging can solve the problem that the battery is difficult to supply power for a long time, greatly reduce costs and promote the concept of sustainable development. And it has high potential to power electronic equipment. Research on how to use solar energy to provide electric energy for electronic equipment, especially when it is inconvenient to replace batteries, has become the focus of many recent studies. Fu *et al.* proposed a new solar bionic underwater glider, which has a variety of motion modes [19]. Hasan *et al.* proposed a doublesided photovoltaic solar panel module for offshore power generation [20].

Inspired by the solar tracking mechanism that the sunflower can adjust the orientation of its flower disk towards the sun to obtain more sunlight, we propose a novel solar tracker for the amphibious robot [21-24] using a foldable solar harvesting mechanism. As shown in Fig. 1, with the attitude adjustment, the robot is able to track the solar position automatically using the robot's local position and time. According to the robot's need, this foldable mechanism is able to open and close, which assists the robot in improving the power harvesting efficiency and reducing water resistance.

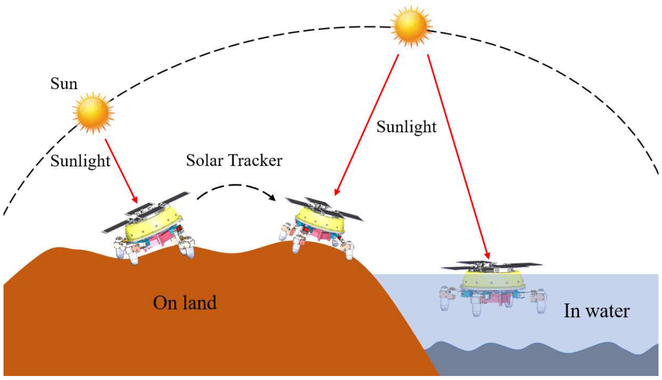

Fig. 1. Schematic diagram of the solar tracker for the amphibious robot. This solar tracker is designed to harvest maximum solar energy in amphibious environments using the foldable solar harvesting mechanism. On land, the robot can adjust the attitude of the solar panels by utilizing four legs. on the surface of the water, the opened solar charging mechanism assists the robot in collecting solar energy.

The reminder of this paper is organized as follows: Section II introduces system overview, i.e., an amphibious robot and the foldable solar harvesting mechanism. In Section III, we present the ADAMS-based simulation of the foldable mechanism. Section IV introduces the control method of the solar tracker. Solar harvesting experiments are conducted with an attitude adjustment and without attitude adjustment in Section V. Finally, Section VI concludes this paper.

II. System Overview

A. *The Amphibious Robot*

In order to improve the working time of the miniature amphibious robots in amphibious environments, we proposed a bioinspired robot with a foldable solar harvesting mechanism. The robot is shown in Fig.1. The robot mainly consists of a sealed cabin, a foldable solar harvesting mechanism, a stereo camera fixed on the sealed cabin, and, a middle aluminium alloy plate, four mechanical legs, and a detachable battery cabin with three batteries containing 13200mAh. The foldable solar harvesting mechanism is mounted on the sealed cabin, and the sealed cabin contains the electronic control system and sensors, such as IMU, temperature sensor and water leakage sensor. On the sealed cabin is a waterproof plug that can make the robot communicate with the remote computer via an optical fiber cable smoothly and steadily. An O-ring is placed between the sealed cabin and middle plant to ensure waterproofing, which makes the robot dive to a maximum of 10m. Using a multi-vectored water-jet propulsion system, the robot can swim in the water. On land, the robot can walk using the legged driving mechanism.

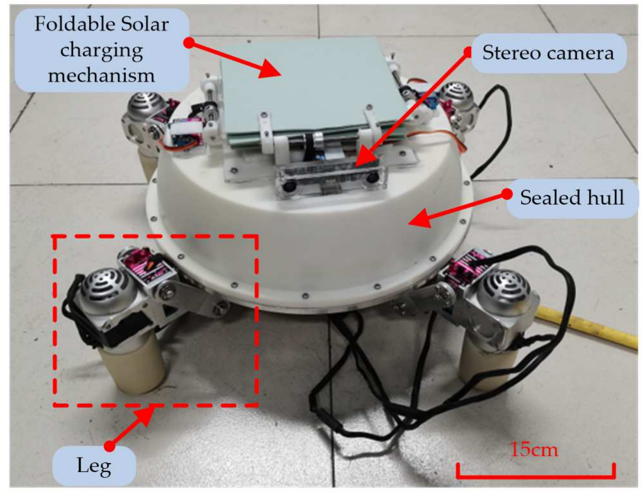

Fig. 2. The overview structure of the developed amphibious robot.

TABLE I
TECHNICAL SPECIFICATION OF THE ROBOT

Items	Parameters
Robot size (LxWxH)	30cmx30cmx30cm
Mass in air	6.5 Kg
Processors	Jetson Nvidia NX, STM32F405
Maximum velocity (cm/s)	5cm/s (on land), 60cm/s (in water)
Communication mode	Wireless mode (2.4GHz, 5GHz)
Power supply	7.4 V lithium batteries (13200mAh)
Operation time	~ 100 min

B. *Fordable Solar Harvesting Mechanism*

In order to maximize solar harvesting efficiency and reduce water resistance, a multi-layer foldable mechanism is designed. This mechanism consists of four panels that are controlled by servo motors. The panels are connected to the servo motors via synchronous belt transmission, and each panel is covered with one solar panel. One solar panel is attached on the robot's sealed shell. Then, five solar panels are used to generate the electric power for the lithium battery. In the process of opening the foldable mechanism, while the first panel spreads out to 90 degrees, the second panel starts to spread out. The rest can be done in the same manner that is able to save time and improve efficiency. Fig. 3(a) and (b) show the open state and close state of the multi-layer foldable mechanism, respectively. While the foldable mechanism is all opened, the solar panel area exposed to the sun is maximized. On land, the robot can adjust its attitude to keep the sun direct beam of light vertical to the face of the solar panels, which also improves the harvesting efficiency of energy. In water, the robot floats, and the solar panels are out of the water to harvest energy. The solar panel is provided by Shenzhen Hong sheng Solar Energy Co., LTD, and the rated charging power of five solar panels is about 10W. When the battery energy was charged or the robot needs to stop charging, the foldable mechanism needs to be closed in the opposite manner.

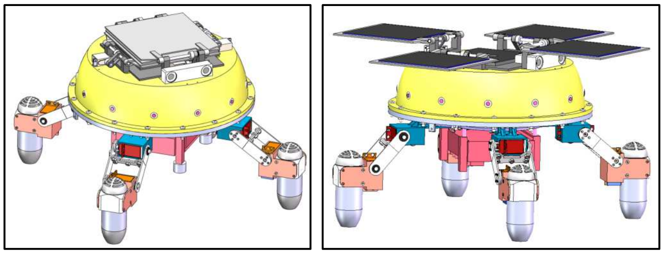

(a) Closing state (b) Opening state

Fig. 3. Opening and closing state of foldable harvesting mechanism.

C. Electronic Control System

The electronic control system of the robot is divided into three parts which include the main control system, the power supply unit (PSU) and the control system of a foldable mechanism serving the solar charging system. As shown in Fig. 4, PSU offers energy to the main control system and the control system of a foldable mechanism by the voltage regulator. Besides, the PSU charge with 10 Watt solar panels using a solar panel charge controller. The main control system, which includes a credit card-sized micro-computer called Jetson Nvidia Xavier NX serves as the main processor, servomotors, thrusters, circuit boards, and multiple onboard sensors are wrapped in the sealed shell. The onboard sensors include a pressure sensor serving water depth monitoring, a leaking detection module, an inertial measurement unit (IMU) and GPS serving for attitudes and position monitoring, and a stereo camera serving for environment capturing. A 32-bit microcontroller (STM32F405) on the circuit boards serves the functions of sensors data acquisition and steering engine control, and this coprocessor is connected to the main processor via UART communication. By controlling the servomotors connected with four legs and water-jet thrusters, the proposed robot is able to swim in the water and walk on land. In the part of the foldable solar system, a 32-bit microcontroller (STM32F103) on the circuit board serves the function of sensors data acquisition and servomotors control. Four servomotors are used to control the foldable solar mechanism. This coprocessor is connected to the coprocessor of the main control system via UART communication.

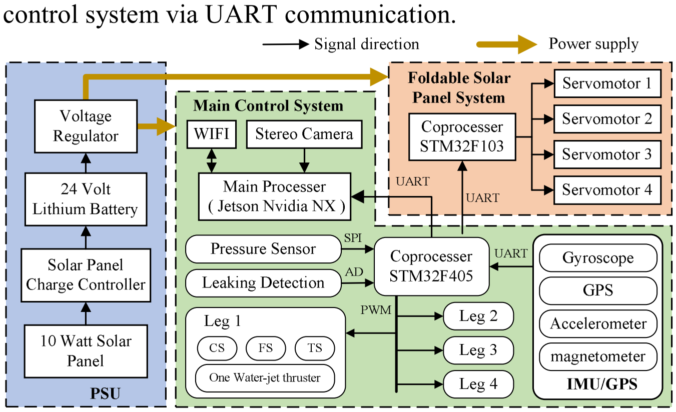

Fig. 4. Electronic control system diagram of the proposed robot.

III. ADAMS-BASED SIMULATION OF FOLDABLE SOLAR HARVESTING MECHANISM

In order to verify the motion effect of the foldable mechanism, we need to transfer the SolidWorks 3D model into the simulation software for dynamic simulation, and obtain the curve of torque, speed and other physical quantities varying with time, so as to facilitate subsequent optimization.

A. Model Building

To verify the stability of the foldable solar harvesting mechanism movement and the rationality of its structural design, it is necessary to create a virtual mechanical structure in ADAMS for simulation. Since the modelling ability of ADAMS is more powerful than that of SolidWorks, we choose to create a model in SolidWorks 3D software, save it as Parasolid (*.xt), and then import it into ADAMS for processing mechanics.

B. Simulation and Optimization

Given that the constraint relationships between components are not preserved when it was imported into ADAMS, it is essential to reset these parameters. During the establishment of ADAMS simulation, factors such as gravitational acceleration and friction are considered to simulate the actual environment as much as possible. The process of establishing the virtual prototype model in ADAMS is as follows:

1) Set the gravitational acceleration of the *Y*-axis (-9.8 m/s^2) vertically downward.

2) According to the density and volume of the whole solar panel, set the mass of the whole solar panel in the simulation software.

3) Establish a fixed pair on the base and each of the four rotating shafts.

4) Establish a rotating pair between the four rotating shafts and the base.

5) Drive the four moving shafts. Since the four solar panels are opened in sequence at intervals of one second, each opening takes two seconds, so the four driving functions are step 1 (time, 0, 0, 2, 180d), step 2 (time,1,0,3,180d), step 3 (time,2,0,4,180d), step 4 (time, 3, 0, 5, 180d).

After completing the above settings, the final model in ADAMS software is shown in Fig. 5.

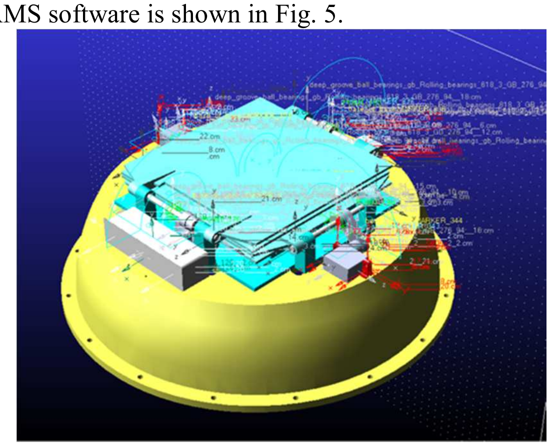

Fig.5. Virtual prototype of the foldable solar harvesting mechanism in the ADAMS platform.

Since the motion laws of the four solar panels are the same, only the motion of the first rotating shaft is analysed. The whole simulation time of the foldable mechanism is 5s. When the simulation ends, the simulation results of torque and angular velocity are generated and shown in Fig.6.

In Fig.6, we see that the change of the torque in the Z-axis direction is stable. At the beginning and end of one solar panel, the force arm is largest and the torque value is almost 0.1N·m. As the simulation progresses, the force arm decreases and the torque decreases. The opening time of the solar panel in the simulation is 1s. The solar panel turns to 90°, and the torque value at this moment is equal to zero. When the solar panel turns from 90° to 180°, the force arm increases, and the torque increases in the opposite direction. In Fig.7, the solar panel makes a uniform circular motion, and the time for complete deployment is 2 seconds, so the angular velocity of the bottom plate is a constant value of 90 degrees/second. From the simulation results, it can be seen that the movement of the bottom plate is stable, and the force is uniform.

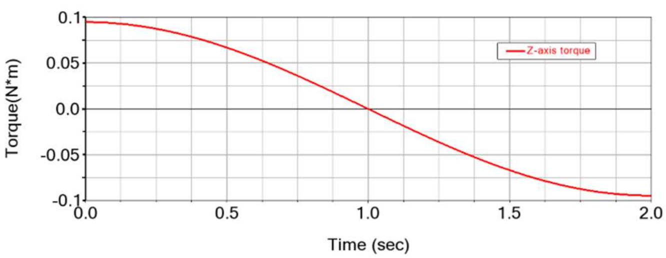

Fig. 6. Simulation results of Z-axis torque.

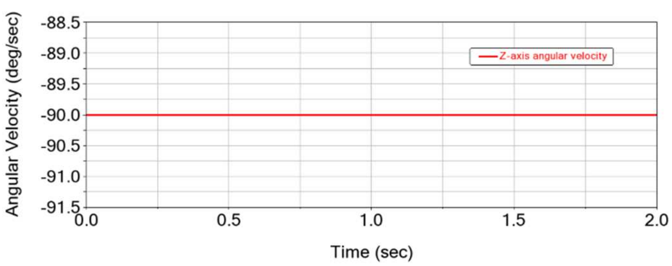

Fig. 7. Simulation results of Z-axis angular velocity.

IV. Solar Tracker Control Method

A. Opening and Closing Control of the Foldable Mechanism

In order to simplify the design as much as possible and reduce the occupied space of the system, the foldable charging design is adopted. The system designs two states of expansion and closure so that the initial area of the solar panel is small and the expansion area is large. The unfolding and closing of the foldable photovoltaic charging system are controlled by controlling four servo motors. When the first solar panel is 90 degrees from the plane of the shell, open the second solar panel, and the third, fourth and so on, as shown in Fig.8. This design reduces the time required to open all mechanisms and improves the solar harvesting efficiency.

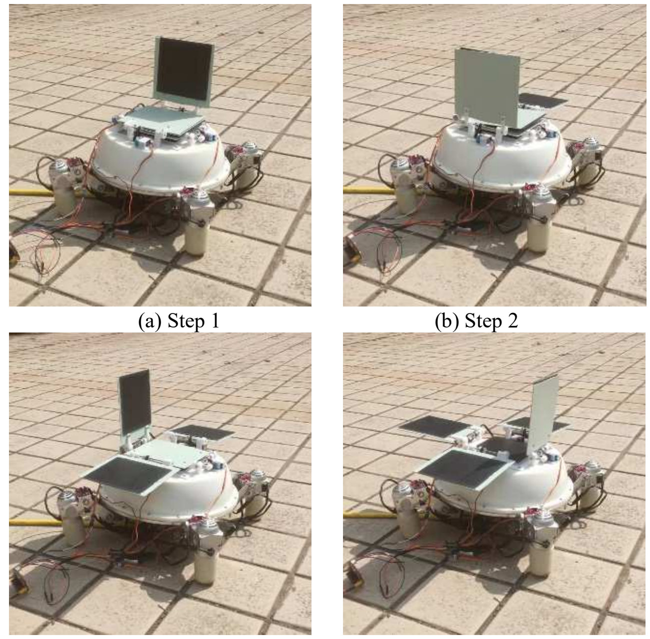

(a) Step 1 (b) Step 2

(c) Step 3 (d) Step 4

Fig. 8. Open and close control of the foldable mechanism.

B. Orientation Control of Solar Panels

For the self-contained amphibious robot, the robot can open the folding solar panel and use the solar energy to charge when it needs to work continuously for a long time. In order to make the solar panel face the sun as much as possible, the robot's body needs to be tilted. Therefore, the gait needs to be adjusted.

In order to make the foldable photovoltaic charging system face the sun as much as possible and improve the utilization efficiency of solar energy, it is necessary to adjust the gait. The Euler angle is set according to the direction of the sun, and the toe position of the leg is controlled according to the Euler angle. In order to keep the position of the robot's toe relative to the ground unchanged, the yaw angle is set to a constant. By pitching and rolling, the robot makes the solar panel face the sun with the largest area. The relationship between Euler angle and toe coordinate is expressed as:

$$\begin{cases} p_z^1 - p_z^4 = \left(p_x^1 - p_x^4\right)\tan\alpha \\ p_z^4 - p_z^3 = \left(p_y^4 - p_y^3\right)\tan\beta \end{cases} \tag{1}$$

where p_z^1 and p_z^4 are the position in Z axis of Left Foreleg and Right Foreleg, α represents the roll, p_z^3 and p_z^4 are the position in Z axis of Right Hind leg and Right Foreleg, β represents the pitch.

The adjusted angle is calculated by Eq. (1) and each leg readjusts the position of the toe according to the calculated angle.

V. Solar Harvesting Experiment

In this section, a series of experiments were conducted to prove the feasibility of the proposed solar tracker by measuring the output power of solar panels at different attitudes.

The experiment is conducted in Harbin, Heilongjiang province, and experimental environment parameters are listed in Table II. As shown in Fig. 9 (a), the initial state of the solar panels was horizontal with the opening state of the foldable mechanism. The sunlight is not vertical to the solar panels and the solar harvesting efficiency is not maximum. As shown in Fig. 9 (b), the amphibious robot adjusted its attitude to face the sun.

TABLE II
THE EXPERIMENTAL ENVIRONMENT PARAMETERS

Items	Parameters
Longitude	126.68285°E
Latitude	45.77584°N
Altitude	148m
Experiment date and time	2022/4/9, 9:00

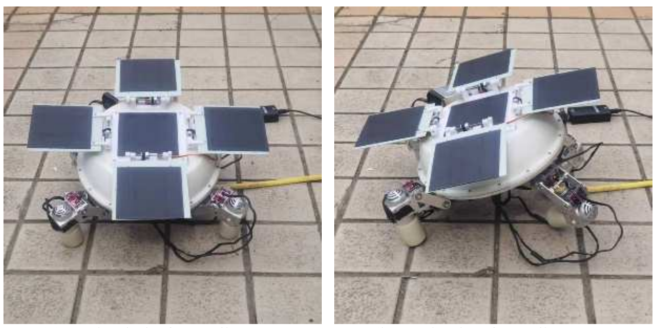

(a) Attitude before adjustment (b) Attitude after adjustment

Fig. 9. Different attitudes on the ground.

In this experiment, in order to evaluate the solar harvesting efficiency varying from the included angle of the sunshine and the panels, the angle between the horizontal plane and the robot attitude varied from 0 degrees to 90 degrees, and the step is 10 degrees. As shown in Fig. 10, the initial power is 3.3169 W, and increases from 0 degrees. The maximum power was reached to 5.3974 W at 60 degrees that keep the solar panels vertical to the sun. Then the power decreased from 60 degrees. The solar energy harvesting efficiency of the solar panels with the attitude facing the sun was improved by 62.4% compared to the horizontal attitude of the solar panels. This experiment verified the proposed solar tracker approach is essential and is able to increase efficiency by 62.4%.

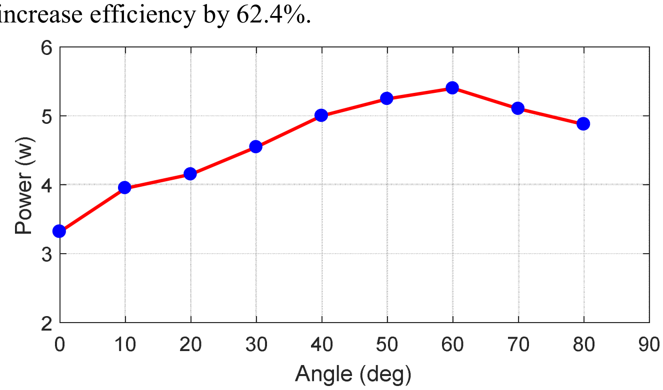

Fig. 10. The output power of solar panels at different attitudes.

IV. CONCLUSION AND FUTURE WORK

This paper proposed a novel solar tracker method with a foldable solar harvesting mechanism for an amphibious robot. This foldable mechanism is optimized using ADAMS simulation, and the driving torques of solar panels are generated for servomotors selection. With the control of four servomotors, four solar panels of the foldable compact mechanism are folded up one by one. Using the required attitude computed by the local position and time of the robot, the robot can adjust the attitude of the solar panels to the sun to obtain the maximum power efficiency. Finally, experiments with the robot attitude adjustment were conducted using the robot prototype. Compared with no attitude adjustment, the solar energy harvesting efficiency is improved by 62.4%, which proved the feasibility of the proposed solar tracker. In the future, we will test the solar energy harvesting efficiency of the robot while working in water.

ACKNOWLEDGMENT

This research is supported by the National High Tech. Research and Development Program of China (No.2015AA043202), the Central Universities of the Ministry of Education of China (3072021CFJ0401, 3072021CF0401), and Graduate Technological Innovation Project of Beijing Institute of Technology (2018CX10022).

REFERENCES

[1] W. S. Hwang, J.H. Ahn, S. Y. Jeong, *et al.*, "Design of piezoelectric ocean-wave energy harvester using sway movement," *Sensors and Actuators A Physical*, vol.260, pp.191-197, 2017.

[2] N. V. Viet, X. Xie, K. M. Liew, *et al.*, "Energy harvesting from ocean waves by a floating energy harvester," *Energy*, vol.112, pp.1219-1226, 2016.

[3] K. Chen, Q. Gao, S. Fang, *et al.*, "An auxetic nonlinear piezoelectric energy harvester for enhancing efficiency and bandwidth," *Appl Energy*, vol.298, no.5, pp.117274, 2021.

[4] S.F. Nabavi, A. Farshidianfar, A. Afsharfard, "Novel piezoelectric-based ocean wave energy harvesting from offshore buoys," *Appl Ocean Res*, vol.76, pp.174-183, 2018.

[5] Y. Peng, Z. Xu, M. Wang, *et al.*, "Investigation of Frequency-up Conversion Effect on the Performance Improvement of Stack-based Piezoelectric Generators," *Renewable Energy*, vol.172, pp.551-563, 2021.

[6] X. Nie, T. Tan, Z. Yan, *et al.*, "Ultra-wideband piezoelectric energy harvester based on Stockbridge damper and its application in smart grid," *Appl Energy*, vol.267, pp.114898, 2020.

[7] M. Masoumi, Y. Wang, "Repulsive magnetic levitation-based ocean wave energy harvester with variable resonance: Modeling, simulation and experiment," *J Sound Vib*, vol.381, pp.192-205, 2016.

[8] J. Prudell, M. Stoddard, E. Amon, *et al.*, "A Permanent-Magnet Tubular Linear Generator for Ocean Wave Energy Conversion," *IEEE Transactions on Industry Applications*, vol.46, no.6, pp.2392-2400, 2010.

[9] W. Li, T.W. Ching, K.T. Chau, "Design and analysis of a new parallel-hybrid-excited linear vernier machine for oceanic wave power generation," *Appl Energy*, vol.208, pp.878-888, 2017.

[10] N. Hodgins, O. Keysan, A. S. Mcdonald, *et al.*, “Design and Testing of a Linear Generator for Wave-Energy Applications,” *IEEE Trans Ind Electron*, vol.59, no.5, pp.2094-2103, 2012.

[11] K. Rhinefrank, E. B. Agamloh, A. von Jouanne, *et al.*, “Novel ocean energy permanent magnet linear generator buoy,” *Renewable Energy*, vol. 31, no.9, pp.1279-1298, 2006.

[12] L. Zhao, H. Zou, G. Yan, *et al.*, “A water-proof magnetically coupled piezoelectric-electromagnetic hybrid wind energy harvester,” *Appl Energy*, vol.239, pp.735-746, 2019.

[13] Y. Na, M.-S. Lee, J. W. Lee, *et al.*, “Wind energy harvesting from a magnetically coupled piezoelectric bimorph cantilever array based on a dynamic magneto-piezo-elastic structure,” *Appl Energy*, vol. 264, pp.114710, 2020.

[14] M.T. Rahman, M. Salauddin, P. Maharjan, *et al.*, “Natural wind-driven ultra-compact and highly efficient hybridized nanogenerator for self-sustained wireless environmental monitoring system,” *Nano Energy*, vol. 57, pp. 256-268, 2019.

[15] Y. Wang, H. Zhang, J. Wu, *et al.*, “Design of a new type underwater glider propelled by temperature difference energy,” *Ship Engineering*, 2009.

[16] S. Zhang, Y. Zhou, M. Xu, *et al.*, “AmphiHex-I: Locomotory Performance in Amphibious Environments with Specially Designed Transformable Flipper Legs,” *IEEE/ASME Transactions on Mechatronics*, vol. 23, no.2, pp.1720-1731, 2018.

[17] H. Liu, L. Shi, S. Guo, *et al.*, “Platform Design for a Natatores-like Amphibious robot,” IEEE International Conference on Mechatronics and Automation, 2018, pp.1627-1632.

[18] H. Xing, L. Shi, K. Tang, *et al.*, “Robust RGB-D Camera and IMU Fusion-based Cooperative and Relative Close-range Localization for Multiple Turtle-inspired Amphibious Spherical Robots,” *Journal of Bionic Engineering*, vol.16, no.3, pp. 442-454, 2019.

[19] K. Fu, P. Wang, B. Sun, *et al.*, “Design, Development and Testing of a New Solar-powered Bionic Underwater Glider with Multi-locomotion Modes,” *OCEANS 2019 - Marseille*, 2019, pp. 1-7, doi: 10.1109/OCEANSE.2019.8867529.

[20] A. Hasan, I. Dincer, “A new performance assessment methodology of bifacial photovoltaic solar panels for offshore applications,” *Energy Convers Manage*, vol.220, pp.112972, 2020.

[21] H. Xing, L. Shi, X. Hou, *et al.*, “Design, modeling and control of a miniature bio-inspired amphibious spherical robot,” *Mechatronics*, vol.77, no.1, pp.1-16, 2021.

[22] H. Xing, S. Guo, L. Shi, *et al.*, “Hybrid locomotion evaluation for a novel amphibious spherical robot,” *Applied Sciences*, vol.8, no.2, pp.156, 2018.

[23] X. Hou, S. Guo, L. Shi, *et al.*, “Improved model predictive-based underwater trajectory tracking control for the biomimetic spherical robot under constraints,” *Applied Sciences*, vol.10, no.22, pp.8106, 2020.

[24] H. Xing, S. Guo, L. Shi, *et al.*, “A Novel Small-scale Turtle-inspired Amphibious Spherical Robot,” *2019 IEEE/RSJ International Conference on Intelligent Robots and Systems (IROS)*, 2019, pp. 1702-1707, doi: 10.1109/IROS40897.2019.8968304.

[25] R. An, S. Guo, L. Zheng, et al., “Uncertain Moving Obstacles Avoiding Method in 3D Arbitrary Path Planning for a Spherical Underwater Robot,” *Robotics and Autonomous Systems*, DOI:10.1016/j.robot.2021.104011.

[26] J. Guo, C. Li, S. Guo, “Study on the Autonomous Multi-Robot Collaborative Control System Based on Spherical Amphibious Robots,” *IEEE Systems Journal*, vol.15, no.4, pp.4950-4957, 2021.

[27] R. An, S. Guo, Y. Yu, et al., “Task Planning and Collaboration of Jellyfish-inspired Multiple Spherical Underwater Robots,” *Journal of Bionic Engineering*, vol.19, pp.643-656, 2022.

[28] J. Guo, C. Li, S. Guo, “Path Optimization Method for the Spherical Underwater Robot in Unknown Environment,” *Journal of Bionic Engineering*, vol.17, pp.944-958, 2020.

[29] J. Guo, C. Li, S. Guo, “A Novel Step Optimal Path Planning Algorithm for the Spherical Mobile Robot Based on Fuzzy Control,” *IEEE Access*, vol.8, pp.1394-1405, 2020.

[30] S. Guo, Y. He, L. Shi, et al., “Modeling and experimental evaluation of an improved amphibious robot with compact structure,” *Robotics and Computer–Integrated Manufacturing*, vol.51, pp.37-52, 2018.

[31] S. Guo, L. Shi, N. Xiao, et al., “A biomimetic underwater microrobot with multifunctional locomotion,” *Robotics and Autonomous Systems*, vol.60, no.12, pp.1472~1483, 2012.

[32] H. Xing, Y. Liu, S. Guo, et al., “A Multi-Sensor Fusion Self-Localization System of a Miniature Underwater Robot in Structured and GPS-denied Environments,” *IEEE Sensors Journal*, vol.21, no.23, pp.27136-27146, 2021.

[33] L. Shi, Y. Hu, S. Su, et al., “A Fuzzy PID Algorithm for a Novel Miniature Spherical Robots with Three-dimensional Underwater Motion Control,” *Journal of Bionic Engineering*, vol.17, no.2, pp.959-969, 2020.

[34] Y. He, S. Guo, L. Shi, et al., “Motion Characteristic Evaluation of an Amphibious Spherical Robot,” *International Journal of Robotics and Automation*, no.206-5399, 2019.